Kinetics and Catalysis, Vol. 45, No. 1, 2004, pp. 141–148. Translated from Kinetika i Kataliz, Vol. 45, No. 1, 2004, pp. 154–161.

Hydrothermal Synthesis of Porous Al_2O_3/Al Metal Ceramics: I. Oxidation of Aluminum Powder and Structure Formation of Porous $Al(OH)_3$/Al Composite

A. I. Rat'ko*, V. E. Romanenkov, E. V. Bolotnikova*, and Zh. V. Krupen'kina***

** Institute of General and Inorganic Chemistry, Belarussian Academy of Sciences, Minsk, 270072 Belarus*

*** Institute for the Advanced Training and Retraining of Personnel, Ministry of Education of the Republic of Belarus, Minsk, Belarus*

Received December 5, 2001; in final form, March 14, 2003

Abstract—The properties of ASD-1 aluminum powder and its oxidation with water at 100°C were studied. It was found that the microstructure of a surface oxide film and the conditions of oxidation significantly affected the dynamics of changes in the pH of the solution and in the degree of aluminum conversion into the hydroxide. Experimental data on the oxidation in combination with electron-microscopic measurements and the determination of adsorption and texture characteristics resulted in the conclusion that colloid-chemical processes, which include the dissolution of aluminum and the formation and precipitation of the hydroxo complexes of aluminum, are fundamental for the synthesis of porous metal ceramics.

INTRODUCTION

Porous oxide–metal composite materials based on aluminum powder synthesized under hydrothermal conditions at 150–250°C exhibit a number of unique properties, and they can be of interest as adsorbents, catalysts, and supports for catalytically active substances [1–11]. For example, Tikhov *et al.* [5, 6] found that a porous composite is promising for the use as a support for catalytically active components in the processes of methane conversion and CO and butane oxidation. Such materials cannot be produced with the use of currently available methods for the formation of porous solids. Moreover, they are free of impurities and catalyst poisons, which are inevitably introduced with the use of ordinary precipitation and impregnation methods [9].

A decrease in the synthesis temperature down to 100°C provides an opportunity to reject autoclave equipment and considerably extends the capabilities of the process. Data on the mechanism of formation of porous composites from aluminum are scanty because the first publications concerning this problem appeared not long ago. However, the knowledge of the mechanism of the synthesis of these materials is of both fundamental and practical importance because it provides an opportunity not only to theoretically interpret this synthesis but also to control the structure and properties of the Al_2O_3/Al system. Tikhov *et al.* [10, 11] believed that a porous composite was formed under hydrothermal conditions in the course of a gas–solid reaction. At the same time, in a number of publications [12–21] on the oxidation mechanisms of dispersed aluminum with water or water vapor, a colloid-chemical character of the formation of a porous solid in the liquid–solid system was assumed. The packing of dispersed aluminum particles is favorable for the adsorption and capillary condensation of water vapor, the formation of water menisci at the sites of contacts between particles, and the formation of the Al–H_2O system [20]. The subsequent hydration reaction of an oxide film that covers the surface of aluminum and the formation of a new pore system by the products of hydrolysis increase its penetrability and provide access for water to the metal surface. An analysis of published data [1–21] suggests that the oxidation of aluminum and the synthesis of composite ceramics are multistage processes. The rates of individual steps and the properties of synthesized materials largely depend on the reaction temperature and the properties of the starting powder. The synthesis of a porous composite consists of the following stages: the hydrolysis of an oxide film on aluminum particles; the hydrolytic reaction of aluminum powder with water; the transfer of metal ions to a solution; the formation and precipitation of the aqua hydroxo complexes of aluminum on the island nuclei of aluminum hydroxide resulting from the hydrolysis of the oxide film; the diffusion of water to the reaction surface and the counterdiffusion of hydrogen and the aqua hydroxo complexes of aluminum through the growing porous layer of aluminum hydroxide followed by precipitation and formation of a continuous porous cover, which is responsible for the formation of a porous solid, on the surface of aluminum particles; and the structural transformations of aluminum hydroxide in the course of the thermal treatment of the cermet synthesized. The rate-limiting step of the synthesis is the slowest step of diffusion, which is responsible for the transfer of the aqua hydroxo complexes of aluminum through the growing

porous hydroxide layer to the outer surface. The subsequent thermal treatment is accompanied by crystal-chemical and structural transformations of the precipitate; these transformations, in turn, can affect the process. Thus, the formation of porous metal ceramics depends on the thermodynamic and kinetic conditions of the synthesis in a condensed phase. Therefore, it is of importance to determine the contributions of each particular steps to the overall process of the formation of a porous Al_2O_3/Al composite, which will be considered in a series of papers.

In this paper, we present the results of a study of the properties of parent aluminum powder and a surface oxygen film and their effects on the occurrence of a chemical reaction and on the texture formation of the $Al(OH)_3$/Al composite.

EXPERIMENTAL

The ASD-1 aluminum powder was obtained by sputtering a melt of commercially pure aluminum with an inert gas in a liquid hydrocarbon. The shape and surface structure of powder particles and the microstructure of the composite synthesized were studied by scanning electron microscopy on a Cam Scan instrument. The particle-size composition of the powder was determined on a TA automatic particle analyzer (Coultronics, France). The specific surface area was measured on a Model 2100 analyzer (Micrometrics, USA). The bulk density was determined in accordance with *GOST* (State Standard) *19440–74*.

In the study of an oxide film on the surface of aluminum particles, various procedures were used in order to obtain reliable and complete information on the structure, phase composition, and thickness of this film. The structure and phase composition of the oxide film were studied by transmission electron microscopy on a UEMV-100V instrument; the interplanar spacing was determined from the diameters of diffraction rings with the use of an IZA-2 comparator. Aluminum particles were prepared for electron-microscopic studies with the use of a carbon replica—a matrix holder, which is transparent to electrons, for an oxide cover from which a metal nucleus was etched in a weakly alkaline solution [22–24]. The oxygen content of the powder was determined on a Model O2A2002 automatic analyzer (Leybold–Hereus, Germany). The concentration of aluminum oxide in the initial powder was calculated from the oxygen content. The thickness of an oxide film on aluminum particles was calculated using the equation [25]

$$\delta = \frac{m}{\rho S}, \quad (1)$$

where m is the oxide content (wt %), ρ is the density of anodically grown amorphous aluminum oxide (3.17 g/cm^3) or the density of γ-alumina (3.32 g/cm^3 [26]), and S is the specific surface area of the powder. The structural transformations of oxide films were studied with the use of thermograms obtained on a Q-1500D instrument (Paulik, Hungary). Aluminum powder was heated in air at a rate of 5 K/min, and the DTA, DTG, and TG curves were recorded simultaneously.

The oxidation of aluminum with water (5 g of powder in distilled water at 100°C) was performed in a beaker with intense stirring using a magnetic stirrer or under batch conditions in a closed mold of corrosion-resistant chromium–nickel steel. The degree of oxidation (α) was determined by measuring the release of hydrogen with a laboratory gasometer on the assumption that aluminum hydroxide is the reaction product. In the course of oxidation with intense stirring, the pH of the solution was monitored with the use of an LP-5 vacuum-tube potentiometer with a glass electrode. The X-ray diffraction analysis of the resulting precipitate was performed on a DRON-3 instrument (CuK_α radiation); identification was performed using reference data.

The macropore-size distribution of the $Al(OH)_3$/Al composite was determined by stereological analysis on a Mini-Magiscan automatic image analyzer using the Genias 26 program. For this purpose, the photographs of fractured sample surfaces obtained on the Cam Scan scanning electron microscope at magnifications of 25, 50, 250, 500, 1000, and 4000 were used. The gas-permeability coefficients and maximum and average macropore sizes were determined in accordance with *GOST* (State Standard) *25283-82* using as test samples disks 35 mm in diameter and 10 mm in thickness.

To determine adsorption and texture characteristics, the adsorption–desorption isotherms of benzene vapor at 20°C were analyzed, which were obtained gravimetrically in a vacuum system with the McBain–Bakr quartz spring balance [27]. The samples were preheated at 140°C in a vacuum for 4 h. Experimental points were measured to the relative pressure $P/P_s = 0.9$; next, extrapolation to $P/P_s = 1.0$ was performed. The specific surface area, average pore radius, and sorption pore volume were calculated from the adsorption isotherms.

The ultimate compression strength of the samples (10×10 mm) was determined in accordance with *GOST* (State Standard) *25282–82* with the use of a universal testing machine at a traverse speed of 1 mm/min.

RESULTS AND DISCUSSION

Structure and Properties of Parent Aluminum Powder

The surface of ASD-1 powder particles is smooth, and the shape is near spherical (Fig. 1a). In contrast to this, PA powders, which were used by Tikhov and coauthors [5–7, 10, 11], as a rule, consist of either coarse particles coated with a layer of small particles (Fig. 1b) or a conglomerate of particles close to each other in size (Fig. 1c); this is characteristic of sputtering an aluminum melt in water. A spherical shape with a smooth surface is most convenient for studying the kinetics and

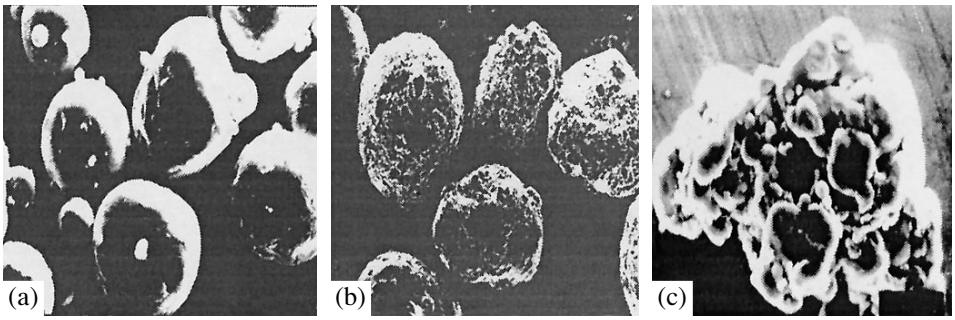

Fig. 1. Particle shapes of (a) ASD-1 and (b, c) PA-4 aluminum powders obtained by sputtering a melt (×2500).

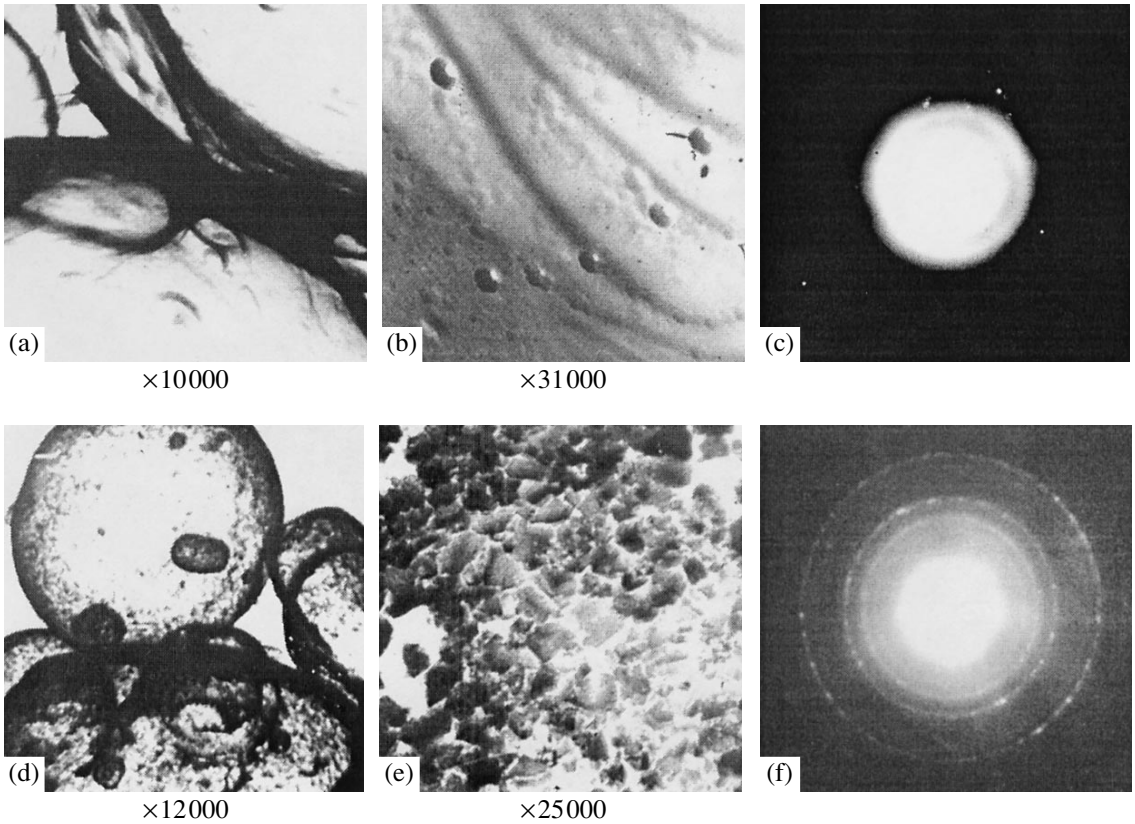

Fig. 2. Microstructure and electron diffraction patterns of oxide films on the particles of (a–c) the parent ASD-1 aluminum powder and (d–f) the ASD-1 powder thermally treated in air at 550°C.

mechanism of formation of a porous composite. This shape makes it possible to study surface morphology changes in the course of a chemical reaction, to identify interparticle contacts, and to analyze the mechanical rupture of samples. Therefore, we used commercially pure ASD-1 powder as a test material; it had a pycnometric density of 2.7 g/cm^3, a bulk density of 1.56 g/cm^3 after shaking, a specific surface area of 0.145 m^2/g, and an average particle size of ~20 μm.

The oxide film on ASD-1 powder particles is transparent to electrons and not ideally smooth. A fine relief as hollows, folds, and convexities (Fig. 2a), which are formed on sputtering the powder because of a difference between the thermal expansion coefficients of the oxide cover and the metal nucleus, can be seen on the film surface. The electron diffraction pattern (fuzzy diffuse rings in Fig. 2b) suggests an amorphous structure of the oxide film due to a high rate of cooling sputtered aluminum droplets (~10^5 K/s [28]), which results in kinetic limitations on the formation and growth of the island nuclei of a crystalline oxide film [29].

In the course of the thermal treatment of the powder in air at 550°C, an amorphous oxide film was completely crystallized for 0.3–0.5 h with the formation of

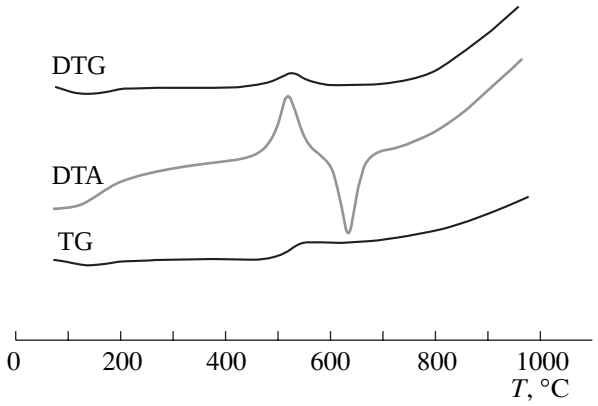

Fig. 3. Thermal analysis curves of the oxidation of the ASD-1 powder in air.

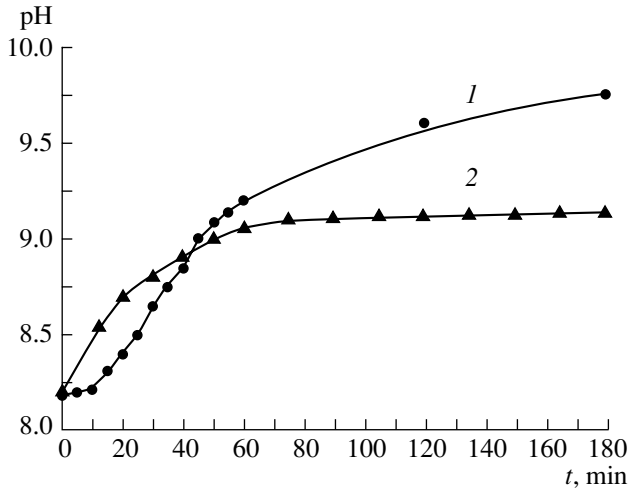

Fig. 4. Kinetic curves of changes in the pH of solution in the oxidation of the ASD-1 aluminum powder in water: (*1*) the initial powder and (*2*) the powder treated in air at 550°C.

γ-Al_2O_3 crystallites, which are opaque to electrons (Figs. 2d, 2e). This was supported by the results of calculating the electron diffraction pattern, which includes pronounced reflections characteristic of the crystal structure (Fig. 2f). The crystallites were irregular polygons in shape and about 100–300 nm in diameter. Narrow regions transparent to electrons were observed at the boundaries between crystallites; it is likely that these regions had another structure.

Some characteristics of an oxide film on the parent ASD-1 powder are given below.

O_2 content, wt %	O_2 content, g/m^2	Al_2O_3 content, g/m^2	Film thickness, nm	Phase composition
0.29	0.02	0.0425	13.4	Amorphous

An analysis of the thermoanalytical curve of the oxidation of ASD-1 powder in air indicates that the weight of the powder somewhat decreased at 120–180°C (Fig. 3, TG curve), and a small endothermic effect due to the removal of physically adsorbed water is visible (DTA curve). In the temperature range 500–700°C, the DTA curve exhibits two extrema, which are indicative of heat release at 520–550°C and heat absorption at 655–670°C. An exothermic peak corresponds to the conversion of the amorphous oxide into crystalline γ-Al_2O_3 [22–24]. Simultaneously, a stepwise increase in the powder weight due to an increase in the rate of oxidation was observed. The transition into a crystalline state was accompanied by an increase in the density of the oxide and, consequently, by a decrease in its volume and specific surface area. As a result, open channels were formed in the oxide film, and the metal nucleus became naked. This nucleus was oxidized by atmospheric oxygen [30] at separate sites to result in a stepwise increase in its weight. After the oxidation of the metal nucleus, the oxide cover became continuous once again, as evidenced by the deceleration of oxidation in the range 570–700°C; this is consistent with published data [31–33].

Oxidation of Aluminum Powder with Water and the Structure of Reaction Products

The kinetic curve of changes in the pH of solution on the oxidation of aluminum powder with an amorphous oxide film is *S*-shaped (Fig. 4, curve *1*), which is characteristic of topochemical processes [34]. At the step of an induction period, the adsorption of H_2O molecules, the hydration of the oxide film [13, 15–18, 20], and the formation of aluminum hydroxide island nuclei took place. Based on a great body of published data [12–21], the overall process can be represented by the following reaction scheme:

$$Al_2O_3 + xH_2O \longleftrightarrow Al_2O_3 \cdot xH_2O, \text{ where } x = 2...3;$$

$$Al_2O_3 \cdot xH_2O + (7 - x)H_2O + 2OH^- \longleftrightarrow 2[Al(OH)_4(H_2O)_2]^-.$$

The hydration of the oxide film affected its homogeneity and continuousness; this is favorable for the access of water to the metal surface and for the occurrence of hydrolytic chemical reactions, which are characterized by an increase in pH [17]:

$$2Al + 6H_2O \longrightarrow 2Al(OH)_3 + 3H_2,$$

$$Al(OH)_3 + 6H_2O \longrightarrow [Al(H_2O)_6]^{3+} + 3OH^-,$$

$$Al_20_3 + 9H_2O \longrightarrow [Al(OH)_3(H_2O)_3],$$

$$[Al(OH)_3(H_2O)_3] + 3H_2O \longrightarrow [Al(H_2O)_6]^{3+} + 3OH^-.$$

The precipitation of the hydroxo complexes and aqua hydroxo complexes of aluminum from solution onto

aluminum hydroxide island nuclei, which were formed in the course of the hydration of the oxide film, was accompanied, depending on the reaction temperature, by the formation of a porous layer of pseudoboehmite

$$(AlOOH \cdot yH_2O)_n + [Al(OH)_4(H_2O)2]^- \longleftrightarrow (AlOOH \cdot yH_2O)_{n+1} + (3 - y)H_2O + OH^-$$

or aluminum hydroxide

$$[Al(H_2O)_6]^{3+} + 3[Al(OH)_4(H_2O)_2]^- \longleftrightarrow 4[Al(OH)_3 \cdot yH_2O)] + 4(3 - y)H_2O.$$

The steps of an induction period and reaction development were absent from the oxidation of powder with a crystalline oxide film, which was formed on heating the parent material in air at 550°C (Fig. 4, curve *2*).

An analysis of the experimental results and published data on pH changes in the course of reaction [17, 20] suggests that the ability of an oxide film to undergo hydrolysis primarily depends on its continuousness and homogeneity. An amorphous oxide film has a homogeneous structure; therefore, there is no clearly defined Al–oxide film interface. At the same time, the lattices of crystalline γ-Al_2O_3 and aluminum are incoherent (lattice parameters are 0.780 and 0.404 nm, respectively), and an interface between γ-Al_2O_3 crystallites and an aluminum support exists. This fact explains the higher penetrability of a crystalline oxide film, although the crystalline oxide film is more stable to the action of water, compared to the amorphous film. As a result, the access of water to the metal surface is facilitated even at the initial step of the process, and a porous precipitate is rapidly formed at the surface of particles.

The degree of oxidation depends on experimental conditions (Fig. 5). The intense stirring of aluminum powder in water is accompanied by the appearance of turbulent flows at the surfaces of spherical particles; this facilitates the transfer of the aqua hydroxo complexes of aluminum to the solution and significantly hinders their precipitation as a porous deposit onto the surface of aluminum. Because of this, ~50% conversion of the metal into the hydroxide was observed even in the first 3.5 h, and a white flocculent precipitate of aluminum hydroxide (according to X-ray diffraction data, this was bayerite) was accumulated at the bottom of the reservoir. Zaporina *et al.* [20], who used electron microdiffraction and thermal analysis, found that bayerite (α-$Al(OH)_3$) was also formed in the reaction of aluminum powder with water vapor at 25°C and a relative humidity of 90%; gibbsite (α-$Al(OH)_3$), pseudoboehmite (γ-AlOOH), and aluminum oxide (γ-Al_2O_3) traces were also detected (endo effects at 283 and 420–523°C). The composition of the reaction products of aluminum with water depends on only the reaction temperature and time [17]. At the step of the development of reaction, the products were X-ray amorphous, and endothermic effects in the region 120–300°C were due to the decomposition of the amorphous hydroxide. A noticeable portion of water was removed at 350–470°C,

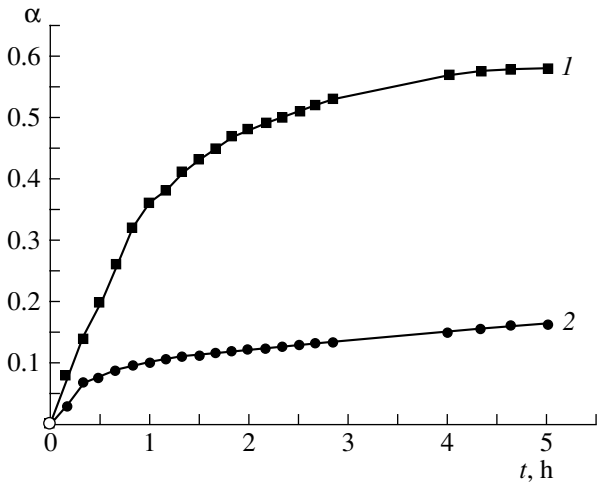

Fig. 5. Changes in the degree of oxidation of aluminum with water depending on reaction time: (*1*) with stirring and (*2*) in a closed mold.

which corresponds to the temperature range of boehmite degradation. Zhilinskii *et al.* [18] detected four endo peaks in the DTA curves of the reaction products of aluminum powder with water; these peaks were due to the removal of physically adsorbed water and the decomposition of the amorphous hydroxide at 100°C and the decomposition of bayerite at 280°C and of pseudoboehmite at 356–370°C. The intensity of the peak due to the decomposition of bayerite increased with increasing reaction temperature, and an additional peak due to the decomposition of pseudoboehmite appeared at 405–410°C.

Pore Structure of the $Al(OH)_3$/Al Composite

The aluminum nucleus included in a porous aluminum hydroxide cover 1–1.5 μm thick can be seen in the electron micrograph of the fracture of the porous $Al(OH)_3$/Al composite synthesized at 100°C for 2.5 h (Fig. 6a). The neighboring cover is devoid of a nucleus, which remained in the adjacent fragment of the fractured sample. The inner part of the cover has a relatively smooth surface, whereas its outer part and the contact zone have developed rough surfaces. This also provides support to the scheme proposed for the formation of a porous composite. This scheme includes the hydrolysis of an oxide surface, the diffusion of the hydroxo complexes of aluminum through a porous bayerite layer, and the deposition of these complexes on the outer surface of the growing bayerite layer. The aggregation of aluminum particles in the course of oxidation for 2.5 h occurred without a noticeable change in their shape and without visible mechanical rupture of the pore structure formed. The resolving power of a scanning electron microscope did not allow us to identify the pore structure of the precipitate in more detail. However, it is believed that the precipitate was formed

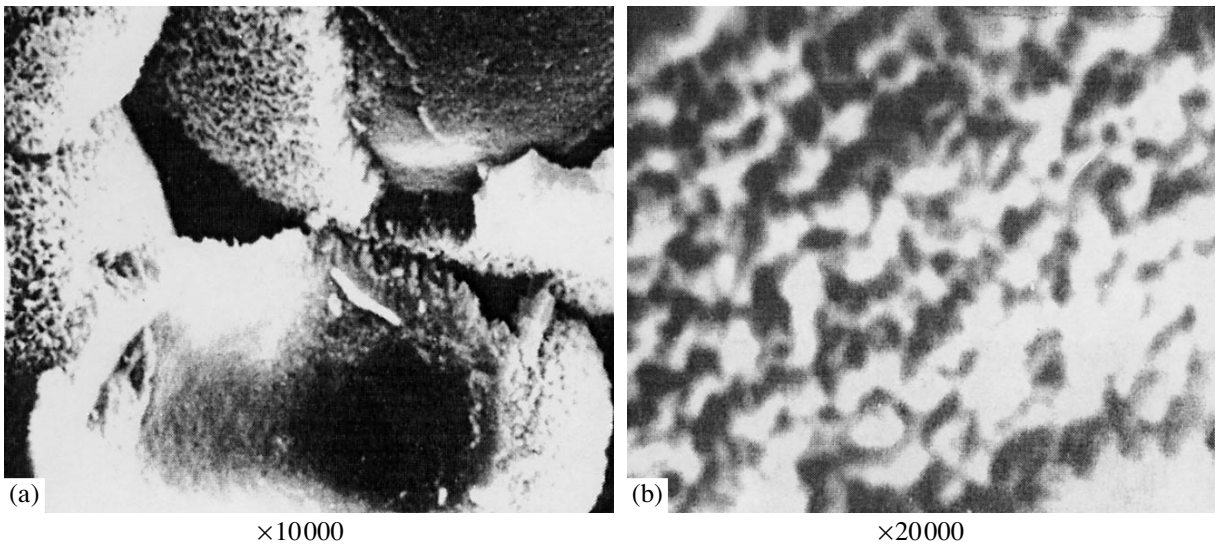

Fig. 6. Microstructures of interparticle contacts and bayerite shells in the porous $Al(OH)_3/Al$ composite: (a) ×10000 and (b) ×20000.

by the packs of bayerite particles joined to each other (Fig. 6b). Ultramacropores in the synthesized material are cavities between packed $Al(OH)_3/Al$ composite particles, which are joined at the sites of contact.

The lattice parameters of aluminum metal and bayerite are significantly different. The incoherence of the lattices explains the low adhesion of the deposited hydroxide to the metal, a higher mechanical strength of the porous cover of bayerite compared with the strength of its joint to the metal support, and the absence of the fragmentary degradation of the cover. In the oxidation of aluminum powder in a closed vessel (mold), the processes of the hydrolysis of aluminum, the precipitation of the hydroxo complexes of aluminum, and the growth of a porous bayerite layer were maximally localized in mother liquor microvolumes adjacent to the surface of particles in the region of interparticle contacts. The aggregation of particles and the formation of a bound disperse solid occurred by the polynuclear deposition of bayerite onto the contact zone and the surface of aluminum particles. However, the formation of a porous bayerite layer facilitated the transfer of the oxidation process to the diffusion region. Therefore, the metal conversion into the hydroxide was no higher than 15–20% even after hydrothermal synthesis for 7.5 h, and the compression strength of the porous composite was no higher than 10–15 MPa. The strength of the material synthesized primarily depended on the amount of the building material: the hydroxo complexes of aluminum deposited in the contact zone. In turn, the amount of the hydroxo complexes depends on the slowest process: the diffusion of these complexes from the reaction surface to the outer surface of the growing porous layer of bayerite.

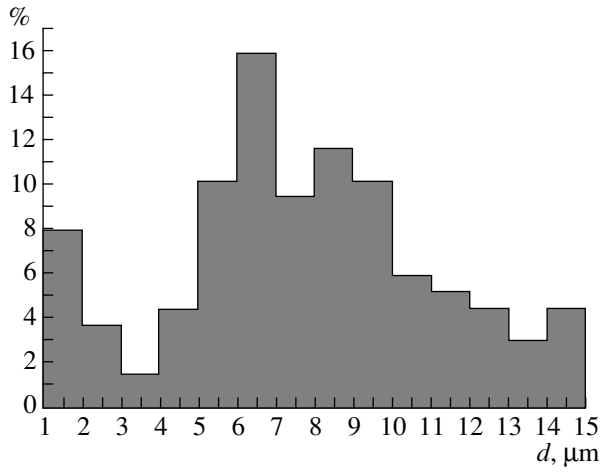

Fig. 7. Bar diagram of ultramacropore-size distribution in the porous $Al(OH)_3/Al$ composite synthesized.

Figure 7 demonstrates the results of the stereological analysis of the pore structure of the $Al(OH)_3/Al$ composite. The material synthesized exhibited a uniform ultramacropore-size distribution because of the spherical shape of powder particles and the homogeneity of their packing. The average particle size of the ASD-1 aluminum powder was ~20 μm; therefore, the average ultramacropore size lay within the range 5–7 μm. Such a ratio is typical of permeable powder materials obtained by powder metallurgy methods. The results of the stereological analysis are consistent with the results obtained in the determination of maximum and average ultramacropore sizes in accordance with *GOST 25283–82*. The gas-permeability coefficient of the material synthesized was equal to $\sim 2.2 \times 10^{-13}$ m^2, which corresponds to the permeability coefficient of a permeable powder material prepared by the sintering of bulk ASD-1 aluminum powder.

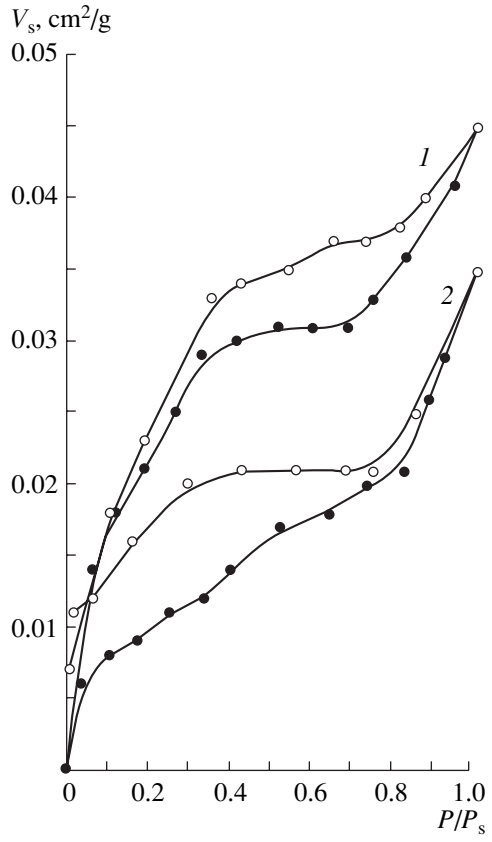

Fig. 8. Benzene adsorption–desorption isotherms at 25°C: (*1*) the precipitate of bayerite and (*2*) the AL$(OH)_3$/Al composite after hydrothermal treatment for 2 h.

Figure 8 demonstrates an isotherm of benzene adsorption–desorption on the precipitate of bayerite formed in the oxidation of aluminum under conditions of intense stirring (curve *1*) and an isotherm of benzene adsorption–desorption on the porous $Al(OH)_3$/Al composite (curve *2*). The isotherm of bayerite exhibits a characteristic hysteresis loop in the region of capillary condensation at a relative pressure $P/P_s > 0.1$, and it is of type 1 according to the IUPAC Classification [35]. A typical distinctive feature of the adsorption isotherm on the porous composite is the nonconvergence of isotherm branches, which can be explained primarily by the occurrence of narrow spots in pores; in the course of desorption, the migration of adsorbate molecules through these narrow spots is difficult [35]. The table summarizes the adsorption and texture characteristics of $Al(OH)_3$/Al composites synthesized by the treatment of aluminum with water for 2–7 h. In the first 2 h of the synthesis, the structure of the material was formed almost completely, and its further changes were insignificant because of diffusion limitations due to the formation of a porous bayerite layer on the surface of the aluminum particles.

Dependence of the adsorption and texture characteristics of the porous $Al(OH)_3$/Al composite on the time of treatment with water

Treatment duration, h	Sorption pore volume, cm^3/g	Specific surface area, m^2/g	Average pore radius, nm
2	0.035	26	2.0
3.5	0.035	28	2.3
5	0.04	34	2.4
7	0.04	36	1.9

Thus, we performed an integrated study of the properties of the ASD-1 aluminum powder and the porous $Al(OH)_3$/Al composite obtained from this powder. The formation of the porous composite under various conditions was studied. The composite was found to consist of isolated aluminum particles covered with a bayerite shell, which exhibits a micropore structure with transport pores between globules.

REFERENCES

1. USSR Inventor's Certificate no. 1444080, *Byull. Izobret.*, 1988, no. 46.
2. Anan'in, V.N., Belyaev, V.V., Romanenkov, V.E., *et al.*, *Vestn. Akad Nauk BSSR. Ser. Khim. Nauk*, 1988, no. 5, p. 17.
3. Azarov, S.M., Romanenkov, V.E., and Smirnova, T.A., *Poroshkovaya Metallurgiya* (Powder Metallurgy), 1988, no. 12, p. 62.
4. USSR Inventor's Certificate no. 1532201, *Byull. Izobret.*, 1989, no. 48.
5. Tikhov, S.F., Sadykkov, V.A., Potapova, Yu.V., *et al.*, *Stud. Surf. Sci. Catal.*, 1998, vol. 118, p. 797.
6. Tikhov, S.F., Sadykov, V.A., Salanov, A.N., *et al.*, *Mater. Res. Soc. Symp. Ser.*, 1998, vol. 497, p. 200.
7. Tikhov, S.F., Salanov, A.N., and Palesskaya, Yu.Vs., *React. Kinet. Catal. Lett.*, 1998, vol. 64, no. 2, p. 301.
8. Rat'ko, A.I., Romanenkov, V.E., Stankevich, M.V., and Smirnov, V.G., *Dokl. Nat. Akad. Nauk Bel., Ser. Khim.*, 2000, no. 1, p. 57.
9. Yakerson, V.I., Dykh, Zh.L., Subbotin, A.N., *et al.*, *Kinet. Katal.*, 1995, vol. 36, no. 6, p. 918.
10. Tikhov, S.F., Fenelonov, V.B., Sadykov, V.A., Potapov, Yu.V., and Salanov, A.N., *Kinet. Katal.*, 2000, vol. 41, no. 6, p. 907 [*Kinet. Catal*. (Engl. Transl.) vol. 41, no. 6, p. 826].
11. Tikhov, S.F. Zaikovskii, V., Fenelonov V.B., Potapova Yu.V., Kolomiichuk V.N., and Sadykov V.A., *Kinet. Katal.*, 2000, vol. 41, no. 6, p. 916 [*Kinet. Catal*. (Engl. Transl.) vol. 41, no. 6, p. 835].
12. Lokenbakh, A.K., Strod, V.V., Lepin', L.K., *et al.*, *Izv. Akad. Nauk Latv. SSR. Ser. Khim.*, 1981, no. 1, p. 50.
13. Lepin', L.K., Lokenbakh, A.K., Zhilinskii, V.V., *et al.*, *Tez. dokl. VIII Vsesoyuz. soveshch. po kinetike i mekhanizmu khimicheskikh reaktsii v tverdom tele* (Proc. VIII All-Union Workshop on the Kinetics and Mechanism of

Chemical Reactions), Chernogolovka: Inst. of Chemical Physics, 1982, p. 166.

14. Zhilinskii, V.V., Lokenbakh, A.K., and Lepin', L.K., *Izv. Akad. Nauk Latv. SSR. Ser. Khim.*, 1982, no. 6, p. 663.
15. Lepin', L.K., Lokenbakh, A.K., and Zhilinskii, V.V., *Fiziko-khimiya i tekhnologiya dispersnykh poroshkov* (Physical Chemistry and Technology of Dispersed Powders), Kiev: IPM AN USSR, 1984, p. 112.
16. Zhilinskii, V.V., Zaporina, N.A., and Romanovska, B.Yu., Abstracts of papers, *Tezisy nauchnykh soobshchenii ural'skoi konferentsii "Poverkhnost' i novye materialy"* (Ural Conf. on Surfaces and New Materials), Sverdlovsk: Ural. Nauchn. Tsentr Akad. Nauk SSSR, 1984, part 1, p. 168.
17. Zhilinskii, V.V., Shcherbakov, V.K., Lokebakh, A.K., and Abele, R.Yu., *Sovershenstvovanie protsessov lit'ya i obrabotki alyuminiya i proizvodstva kremniya* (Advances in the Process of Casting and Processing of Aluminum and Silicon Production), Ostanin, Yu.A., Ed., Leningrad: VAMI, 1985, p. 45.
18. Zhilinskii, V.V., Lokenbakh, A.K., and Lepin', L.K., *Izv. Akad. Nauk Latv. SSR. Ser. Khim.*, 1986, no. 2, p. 151.
19. Zhilinskii, V.V., Lokenbakh, A.K., and Lepin', L.K., *Izv. Akad. Nauk Latv. SSR. Ser. Khim.*, 1986, no. 2, p. 157.
20. Zaporina, N.A., Ushpele, I.P., Romanovska, B.Yu., *et al.*, *Intersifikatsiya proizvodstva produktsii iz alyuminiya, kremniya i ikh splavov* (Intensification of Production Based on Aluminum, Silicon, and Their Alloys), Leningrad: VAMI, 1987, p. 17.
21. Zhilinskii, V.V. and Lokenbakh, A.K., *Izv. Akad. Nauk Latv. SSR. Ser. Khim.*, 1988, no. 5, p. 622.
22. Romanenkov, V.E., *Cand. Sci. (Eng.) Dissertation*, Minsk: Byelorussian State Polytechnic Academy, 1996.
23. Vityaz', P.A., Sheleg, V.K., Anan'in, V.N., *et al.*, *Dokl. Akad. Nauk BSSR. Ser. Khim.*, 1986, vol. 30, no. 3, p. 240.
24. Reut, O.P. and Romanenkov, V.E., *Vesti Nat Akad. Nauk Bel., Ser. Fiz.-Tekh. Nauk*, 1998, no. 1, p. 11.
25. Nechitailov, A.P., Plakhotnikova, N.A., and Shitova, T.A., in *Lit'e i obrabotka alyuminiya* (Casting and Processing of Aluminum), Leningrad: VAMI, 1977, no. 99, p. 96.
26. Thompson, G.E., Shimizu, K., and Wood, G.C., *Nature*, 1980, vol. 286, p. 471.
27. *Eksperimental'nye metody v adsorbtsii i molekulyarnoi khromatografii* (Experimental Methods in Adsorption and Molecular Chromatography), Kiseleva, A.V. and Dreving, V.P., Eds., Moscow: Mos. Gos. Univ., 1973.
28. Singer, A.R.E., Coombs, J.S., and Leatham, A.G., *Modern Dev. Pov. Met.*, 1974, vol. 34, p. 263.
29. Ananin, V.N., Vityaz, P.A., Glukhova, N.P., *et al.*, *React. Kinet. Catal. Lett.*, 1985, vol. 27, no. 2, p. 393.
30. Anan'in, V.N., Romanenkov, V.E., and Smirnova, T.A., *Dokl. Akad. Nauk BSSR*, 1987, vol. 31, no. 9, p. 818.
31. Shevchenko, V.G., Bulatov, M.A., Kononenko, V.I., *et al.*, *Poroshkovaya metallurgiya* (Powder Metallurgy), 1988, no. 2, p. 1.
32. Shevchenko, V.G., Kononeko, V.I., Latosh, I.N., *et al.*, *Poroshkovaya metallurgiya* (Powder Metallurgy), 1991, no. 5, p. 80.
33. Il'in, A.P. and Proskurovskaya, L.T., *Poroshkovaya metallurgiya* (Powder Metallurgy), 1990, no. 9, p. 32.
34. Panchenkov, G.M. and Lebedev, V.P., *Khimicheskaya kinetika i kataliz* (Chemical Kinetics and Catalysis), Moscow: Khimiya, 1985.
35. Gregg, S.J. and Sing, K.S.W., *Adsorption, Surface Area, and Porosity*, London: Academic, 1967.